

Investigation of Surface Potential Distributions of Phosphorus-doped n-BaSi₂ Thin-Films by Kelvin Probe Force Microscopy

Daichi Tsukahara¹, Masakazu Baba¹, Ryota Takabe¹, Kaoru Toko¹, and Takashi Suemasu^{1,2*}

¹University of Tsukuba, Institute of Applied Physics, Tsukuba, Ibaraki 305-8573, Japan

²JST-CREST, Tokyo, Japan

E-mail: suemasu@bk.tsukuba.ac.jp

(Received July 18, 2014)

We investigated the surface potential distributions around grain boundaries (GBs) in phosphorus (P)-doped n-BaSi₂ thin-films by Kelvin probe force microscopy (KFM) and the crystal planes constituting GBs by transmission electron microscopy (TEM). By KFM measurements, it was found that the GBs in P-doped n-BaSi₂ are different from those in undoped BaSi₂; undoped n-BaSi₂ has a downward band bending around the GBs with barrier heights of approximately 30 meV. In contrast, P-doped n-BaSi₂ has an upward band bending with barrier heights of approximately 15 meV. TEM observation revealed that most of the GBs in P-doped BaSi₂ are composed of BaSi₂ (011)/(0-11) planes. This result is the same as that in undoped BaSi₂.

1. Introduction

BaSi₂ has an ideal band gap of approximately 1.3 eV and a large absorption coefficient of $3 \times 10^4 \text{ cm}^{-1}$ at 1.5 eV [1,2]. Accordingly we consider BaSi₂ as a new candidate for thin-film solar cell materials. By molecular beam epitaxy (MBE), BaSi₂ can be grown on Si(111) substrates with three epitaxial variants rotated by 120° with each other around the surface normal [3,4]. Thus, these films are polycrystalline and contain many grain boundaries (GBs). The grain size of BaSi₂ films grown on Si(111) reached a maximum of approximately 4 μm [5]. Generally, GBs are considered to be defective and thus have negative influence on solar cell performance. Therefore, we investigated the potential profiles across GB in undoped n-BaSi₂ on Si(111) and found that it had a downward band bending with small potential barrier heights of approximately 30 meV for holes at GBs. Therefore, the GBs are thought not to deteriorate the minority-carrier transport in the n-BaSi₂ [6]. In this work, we formed phosphorus(P)-doped BaSi₂ and evaluated the surface potential variations around the GBs using Kelvin probe force microscopy (KFM). We also examined the crystal planes at the GBs by transmission electron microscopy (TEM). According to our previous studies, P-doped BaSi₂ showed n-type conductivity [7].

2. Experiment

A 200 nm-thick P-doped n-BaSi₂ film was grown on Si(111) using MBE referring to our previous reports[7]. An ion-pumped MBE system equipped with standard Knudsen cells for Ba, and P, and an electron-beam evaporation source for Si was used for the growth. For P-doped BaSi₂, crystalline GaP was used for supplying P. The temperature of GaP was fixed at 550 °C and the substrate temperature was also set at 550 °C. The crystalline quality of the grown films were characterized by reflection high-energy electron diffraction (RHEED) and X-ray diffraction (XRD). The doping of P atoms in the grown layers was confirmed by secondary ion mass spectrometry (SIMS). Reference samples with a controlled number of P atoms doped in BaSi₂ have not yet been

prepared. The surface potentials were characterized by KFM (Shimazu SPM-9600) and the crystal planes constituting GBs were examined by TEM.

3. Experimental Results and Discussions

We observed the diffraction peaks of [100]-oriented BaSi₂ in the θ -2 θ XRD pattern and the spotty RHEED pattern. These results indicate that *a*-axis-oriented P-doped BaSi₂ was grown on Si(111). The electron concentration, n , was $n = 4.0 \times 10^{17} \text{ cm}^{-3}$ by Hall measurements. SIMS measurements revealed that the doping of P atoms in the grown layers was confirmed. Ga atoms were found to be also included. According to Ref. [8], Ga doping forms n-type BaSi₂. However, the Ga concentration was smaller by 3 orders of magnitudes than P. Thus, the influence of Ga is thought to be negligibly small.

Figure 1 shows the $3 \times 3 \mu\text{m}$ AFM topographic and KFM potential images with cross sectional profiles along white broken line AA' in the P-doped BaSi₂. Both images were taken in the same area. In these profiles, the position of GBs are indicated by colored lines. In Fig. 1, we see that the electrostatic potentials at the GBs were smaller than those of grain interiors. This result means that the GBs are negatively charged compared with the grain interiors, suggesting that the upward band bending occurred around the GBs.

Next, we evaluated the potential barrier height ΔE_{GB} at GBs by the following Eq. (1)

$$\Delta E_{\text{GB}} = -e(V_{\text{GB}} - V_{\text{G,ave}}), \quad (1)$$

where V_{GB} is the electrostatic potential at GBs, $V_{\text{G,ave}}$ is the average potential of inner parts of two adjoining grains, and e is the elementary charge. We applied Eq. (1) to 37 GBs. The histogram of barrier heights is shown in Fig. 2. The barrier height for electrons ranges from 5 to 35 meV, and we see that the GBs with barrier heights of approximately 15 meV for electrons are dominant. In undoped n-BaSi₂ ($n = 5.0 \times 10^{15} \text{ cm}^{-3}$ [2]), the average barrier height at GBs is approximately 30 meV for holes. Therefore, the characteristics of GBs changed greatly by adding P atoms. From the results mentioned above, the band structure around GBs is determined as shown in Fig. 3. There seems to be two possibilities to explain this result; (1) the Fermi level, E_f , is almost pinned at GBs and E_f approaches the bottom of the conduction band, E_c , in the BaSi₂ grains because of P doping. This may lead to the upward band bending as shown in Fig. 3 as in heavily Sb-doped n-BaSi₂[9], (2) the crystal planes which form GBs changed by P doping and thereby the sign of potential barrier height at GBs with respect to the BaSi₂ grains changed from undoped ones. In order to clarify the crystal planes at the GBs in P-doped BaSi₂, TEM observation was performed [4].

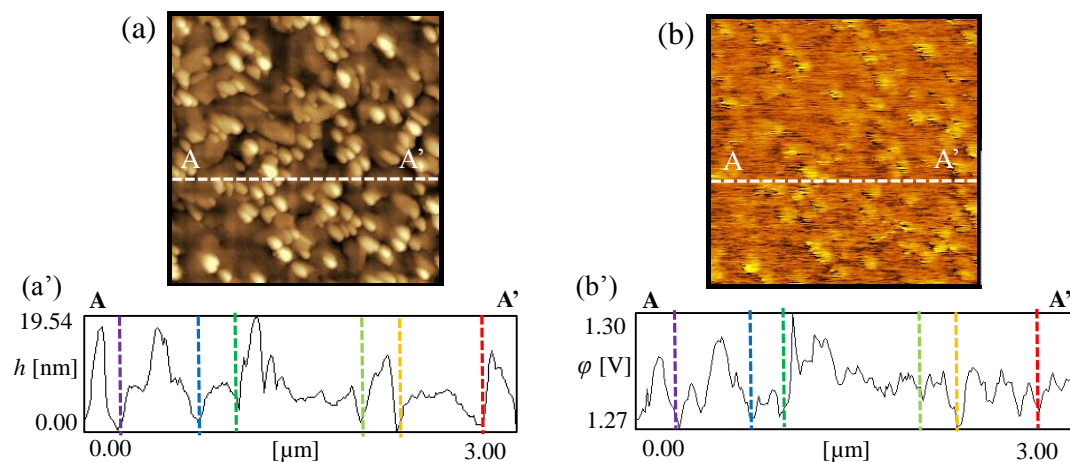


Fig. 1. (a) Surface topographic and (b) surface potential distribution images of P-doped BaSi₂ observed in the same area. (a') and (b') are the cross sectional profiles along dotted line AA' in (a) and (b), respectively.

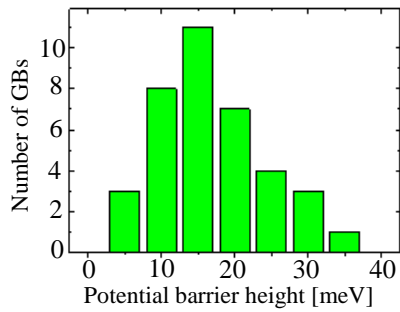


Fig. 2. Histogram of potential barrier height at GBs for P-doped BaSi₂.

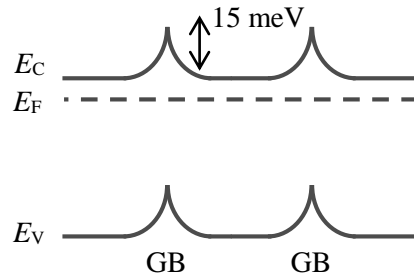


Fig. 3. Band structure around the GBs for P-doped BaSi₂.

A bright-field plan-view TEM observation of the P-doped BaSi₂ was first carried out. The incident electron beam direction was almost parallel to the BaSi₂ [100] zone axis. From selected-area electron diffraction (SAED) pattern, we found that the GBs were composed of (011) and/or (002) plane like in undoped BaSi₂. It was difficult to distinguish the diffraction of (011) from that of (002) in the SAED pattern because their lattice spacings are almost the same. Thus, we next performed dark-field (DF) plan-view TEM observations with a two-beam diffraction condition and observed only BaSi₂ (00n) planes with the diffraction vectors \mathbf{g} set to be $\langle 004 \rangle$. DF plan-view TEM images under a two-beam diffraction condition are shown in Fig. 4. Bright domains in each figure corresponds to one of the three epitaxial variants. We see that the liner GBs are composed of mostly BaSi₂ (011)/(0-11) planes. This result is the same as that in undoped BaSi₂, meaning that the crystal planes which form GBs did not change by P doping. We therefore suppose that the upward band bending shown in Fig. 3 is caused by not the change of the planes but the movement of E_f in the inner part of BaSi₂ grains [9]. Further studies are mandatory to discuss further.

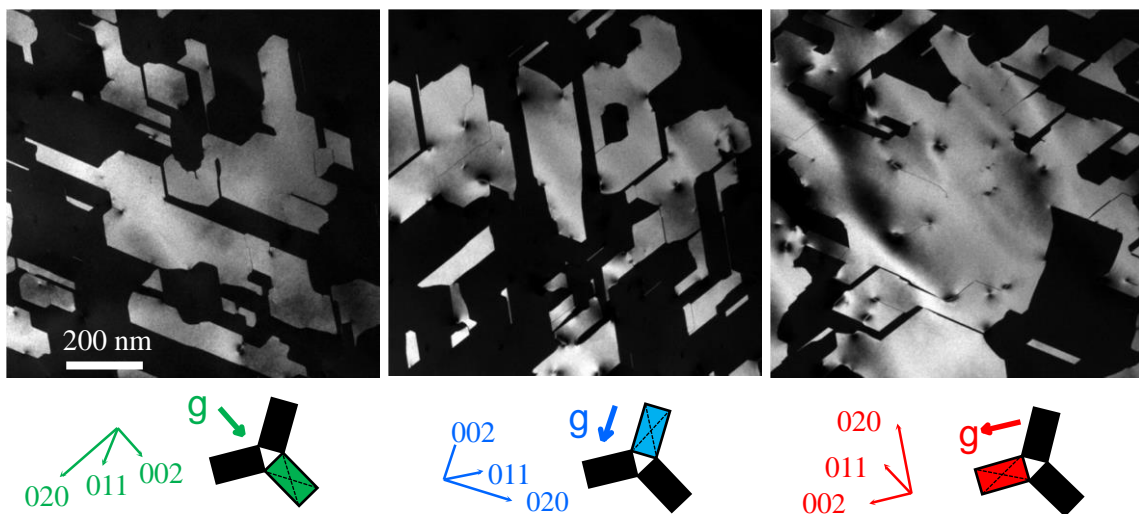


Fig. 4. DF plan-view TEM images under a two-beam diffraction condition. The diffraction vector \mathbf{g} was set to be $\langle 004 \rangle$ for each BaSi₂ epitaxial variant. In each figure, one of the three epitaxial variants is observed bright.

4. Conclusion

We determined the position of GBs in P-doped BaSi₂ on Si(111) by AFM and investigated the surface potential distribution around the GBs by KFM. Although the downward band bending was observed in undoped n-BaSi₂, the upward band bending was confirmed around GBs in P-doped BaSi₂. The potential barrier height was about 15 meV for electrons. From the DF plan-view TEM observation, we found that the GBs consisted mostly of (011) and (0-11) planes, which is the same as in undoped BaSi₂. We therefore suppose that the upward band bending occurred because $E_c - E_f$ became smaller in P-doped n-BaSi₂ than in undoped n-BaSi₂ while E_f was almost pinned at the GBs

Acknowledgment

This work was financially supported by the Japan Science and Technology Agency (JST/CREST).

References

- [1] K. Toh, T. Saito, and T. Suemasu, Jpn. J. Appl. Phys. **50** (2011) 068001.
- [2] K. Morita, Y. Inomata, and T. Suemasu, Thin Solid Films **508** (2006) 363.
- [3] Y. Inomata, T. Nakamura, T. Suemasu, and F. Hasegawa, Jpn. J. Appl. Phys. **43** (2004) L478.
- [4] M. Baba, K. Toh, K. Toko, N. Saito, N. Yoshizawa, K. Jiptner, T. Sekiguchi, K. O. Hara, N. Usami, and T. Suemasu, J. Cryst. Growth, **348** (2012) 75.
- [5] M. Baba, K. Nakamura, W. Du, M. A. Khan, S. Koike, K. Toko, N. Usami, N. Saito, N. Yoshizawa, and T. Suemasu, Jpn. J. Appl. Phys. **51** (2012) 098003.
- [6] M. Baba, S. Tsurekawa, K. Watanabe, W. Du, K. Toko, K. O. Hara, N. Usami, T. Sekiguchi, and T. Suemasu, Appl. Phys. Lett. **103** (2013) 142113.
- [7] R. Takabe, M. Baba, K. Nakamura, W. Du, M. A. Khan, S. Koike, K. Toko, K. O. Hara, N. Usami, and T. Suemasu, Phys. Stat. Sol. C **10** (2013) 1753.
- [8] M. Kobayashi, K. Morita, and T. Suemasu, Thin Solid Films **515** (2007) 8242.
- [9] D. Tsukahara, M. Baba, S. Honda, Y. Imai, K. O. Hara, N. Usami, K. Toko, J. H. Werner, and T. Suemasu, J. Appl. Phys. **116** (2014) 123709.